AWARD NUMBER: W81XWH-13-1-0112

TITLE: In Vivo Imaging of Cortical Inflammation and Subpial Pathology in Multiple Sclerosis by Combined PET and MRI

PRINCIPAL INVESTIGATOR: Caterina Mainero, MD, PhD

CONTRACTING ORGANIZATION: Massachusetts General Hospital
Boston, MA 02114

REPORT DATE: September 2016

TYPE OF REPORT: Annual

PREPARED FOR: U.S. Army Medical Research and Materiel Command
Fort Detrick, Maryland 21702-5012

REPORT DOCUMENTATION PAGE

Form Approved
OMB No. 0704-0188

1. REPORT DATE	2. REPORT TYPE	3. DATES COVERED
September 2016	Annual	09/01/2015-08/31/2016

4. TITLE AND SUBTITLE
In Vivo Imaging of Cortical Inflammation and Subpial Pathology In Multiple Sclerosis by Combined PET and MRI.

5a. CONTRACT NUMBER
W81XWH-13-1-0112

5b. GRANT NUMBER
MS#120086

5c. PROGRAM ELEMENT NUMBER

6. AUTHOR(S)
Caterina Mainero, MD, PhD

E-Mail: caterina@nmr.mgh.harvard.edu

5d. PROJECT NUMBER

5e. TASK NUMBER

5f. WORK UNIT NUMBER

7. PERFORMING ORGANIZATION NAME(S) AND ADDRESS(ES)
Massachusetts General Hospital
Boston, MA 02114

8. PERFORMING ORGANIZATION REPORT NUMBER

9. SPONSORING / MONITORING AGENCY NAME(S) AND ADDRESS(ES)
U.S. Army Medical Research and Materiel Command
Fort Detrick, Maryland 21702-5012

10. SPONSOR/MONITOR'S ACRONYM(S)

11. SPONSOR/MONITOR'S REPORT NUMBER(S)

12. DISTRIBUTION / AVAILABILITY STATEMENT
Approved for Public Release; Distribution Unlimited

13. SUPPLEMENTARY NOTES

14. ABSTRACT
Post-mortem studies in multiple sclerosis (MS) suggested that cortical demyelinating lesions, which are hardly detected in vivo on conventional magnetic resonance imaging (MRI) scans, are an important correlate of disability, and are driven by organized neuroinflammation with the activation of microglia. Activated microglia up-regulate expression of the 18kDa translocator protein (TSPO), which can be imaged in vivo with [-^{11}C-PBR28, a second generation TSPO ligand.
In this study, we combined ultra-high field 7 Tesla (T) MRI, which has demonstrated greater sensitivity to cortical lesions than conventional MRI, with ^{11}C-PBR28 positron emission tomography (PET) imaging of activated microglia to assess whether more severe structural cortical pathology in MS is related to the presence of neuroinflammation. We found that, relative to healthy controls, MS subjects exhibited abnormally high ^{11}C-PBR28 binding across the brain, the greatest increases being in cortex and cortical lesions, deep gray matter (GM) but also and in normal appearing white matter (NAWM). The observed increased ^{11}C-PBR28 binding in cortex, deep GM, and NAWM correlated with neurological disability and impaired cognitive performance; in the cortex it correlated with cortical demyelination as measured by 7T MRI. Quantification of TSPO levels in MS could prove a sensitive tool for evaluating *in vivo* neuroinflammation and its correlates.

15. SUBJECT TERMS
Multiple sclerosis; cortex; cortical lesions; neuroinflammation; microglia; ^{11}C-PBR28 PET imaging; ultra-high field MRI; neurological disability, cognition, deep gray matter, normal appearing white matter, neurdegeneration.

16. SECURITY CLASSIFICATION OF:			17. LIMITATION OF ABSTRACT	18. NUMBER OF PAGES	19a. NAME OF RESPONSIBLE PERSON
					USAMRMC
a. REPORT	b. ABSTRACT	c. THIS PAGE			19b. TELEPHONE NUMBER *(include area code)*
Unclassified	Unclassified	Unclassified	Unclassified	24	

Table of Contents

Page 1

1. Introduction

Multiple sclerosis (MS) is an immune-mediated chronic disease of the central nervous system (CNS), pathologically characterized by inflammation, demyelination and neurodegeneration, and with great variability in the clinical course of individual subjects.

Histopathological examinations of MS brains indicated that cortical demyelinating lesions are potential biomarkers of MS progression. Since cortical lesions appeared topographically related to focal meningeal inflammation in some pathological studies, it has been hypothesized that cortical demyelination in MS may be driven by organized meningeal inflammation through the activation of microglia, accompanied by a decreasing gradient of demyelination away from the pial surface (Magliozzi et al, Brain 2007; Ann Neurol 2010).

Histopathological evidence that the cortex can be the site of inflammatory demyelinating lesions near the time of MS onset (Lucchinetti et al, New Engl J Med 2011) further supports the existence of an early pathological process that primarily targets the cortex, independently from white matter (WM).

Although largely undetected on conventional magnetic resonance imaging (MRI) scans, cortical lesions have been imaged in vivo with improved sensitivity and spatial specificity at ultra high-field 7 Tesla (T) MRI. We developed a reproducible surface-based analysis for mapping cortical T_2* relaxation rates (quantitative- T_2* or q-T_2*) as a function of cortical depth from ultra high-resolution gradient echo 7 T MRI scans. This technique has proved useful for studying the laminar architecture of the cortex in vivo, and for characterizing cortical pathological abnormalities in MS associated with changes in cortical myelin and/or iron concentration.

The purpose of this project is to evaluate inflammation and structural tissue changes in the cortex of patients with relapsing-remitting (RR) MS by combining advanced MR studies at 7 T MRI, to measure cortical lesions and diffuse subpial pathology, with positron emission tomography (PET) using the 18kDa translocator protein (TSPO)-targeting radioligand [^{11}C]-PBR28 to directly quantify microglia activation. Activated microglia/macrophages upregulate expression of the TSPO, which can be imaged in vivo by selective PET-TSPO radioligands, of which ^{11}C-PK11195 is the best known. ^{11}C-PBR28 is a second-generation TSPO PET tracer with ~80 times more specific binding than ^{11}C-PK1119520, and good reproducibility. In experimental studies inflammation-induced microglial activation determined ^{11}C-PBR28 signal increase, confirmed pathologically to mainly result from microglia binding22

The overall working hypothesis is that patients with MS will show areas of cortical inflammation, topographically associated with the presence of structural cortical abnormalities (lesions) and neurodegeneration (cortical tissue loss), as suggested by post-mortem examinations. The ability to quantify in vivo MR tissue changes at different cortical depths from the pial surface, across the whole cortical mantle, and to couple these measurements with assessment of neuroinflammation, can provide insights on the biological basis of cortical degeneration in MS. This, in turn, could help to predict aggressive forms of the disease that can be susceptible to earlier and more specific therapies.

The in vivo study of the inflammatory and degenerative components of cortical disease in MS can have major implications for diagnosing, and understanding the pathogenesis of disease progression in MS.

2. Keywords

1. Multiple sclerosis (MS)
2. Relapsing-remitting (RR)
3. Cortical lesions
4. 7 Tesla magnetic resonance imaging (7T MRI)
5. White matter (WM) lesions
6. Normal appearing white matter (NAWM)
7. Positron emission tomography
8. ^{11}C-PBR28
9. Microglia
10. Macrophages
11. Inflammation
12. Standard uptake values (SUV)
13. Normalized standard uptake values (SUVR)
14. Volume of distribution (VT)
15. Volume of distribution ratio (DVR)
15. Expanded disability status scale (EDSS)
16. Thalamus
17. Deep gray matter (DGM)
18. Cognition

3. Accomplishments.

Main objectives

The major goals of the project were: i) to assess in patients with MS microglia activation in the cortex, as measured by ^{11}C-PBR28 binding, and its association with subpial pathology and cortical lesions; ii) to determine in MS subjects the relationship between cortical inflammation, as measured by cortical ^{11}C-PBR28 binding, disability and cognitive performance.

Specific accomplishments

We consented and enrolled in the study 20 RRMS subjects, which were then genotyped for the Ala147Thr polymorphism in the TSPO gene. Only high- and mixed-affinity binders (HAB, MAB) underwent subsequent study procedures. Seven age-matched healthy controls (HC) were also consented and included in the study for 7 T MRI protocols.

Fourteen RRMS subjects have completed all study procedures, which include 90 min MR-PET after injection of ^{11}C-PBR28, 7 Tesla T2* imaging for cortical lesion segmentation, clinical assessment of neurological disability (EDSS, 9-hole peg test, ambulation index) and cognitive functions (information processing speed, memory, executive function).

One patient was excluded because resulted as low-affinity binder, one subject withdrew from the study, one was later excluded because it resulted that the patient was assuming benzodiazepines that interfere ^{11}C-PBR28 uptake, 2 RRMS subjects need to complete the study. Given that the targeted enrollment has not been completed yet, the main aims of the study have been assessed in 12 RR MS cases, which have also been compared to 15 subjects with a more advanced stage of the disease, namely secondary-progressive (SPMS), recruited as part of another study funded by the MS National Society. The results reported below are thus obtained from a cohort of 27 MS subjects (12 RRMS and 15 SPMS) and 14 age and affinity matched HC.

Methods

All subjects underwent a 90-minutes ^{11}C-PBR28 MR-PET scan on a Siemens simultaneous MR-PET system, BrainPET, a brain PET scanner operating in the bore of a 3T whole-body MR system equipped with an 8-channel head coil. The spatial resolution of the BrainPET (<3 mm in the center of the field of view) is superior to that of any other whole-body PET scanner, because of the smaller size of scintillator crystals and of the scanner diameter, which minimizes the non-colinearity effect. Within one week from MR-PET, 24 MS subjects underwent 7T MRI on a Siemens scanner using a 32-channel head coil. Three subjects were excluded due to the presence of implants not approved for 7T. The 7T protocol included acquisition of 2D-fast low-angle shot-T2* spoiled single- and/or multi-echo images covering the supratentorial brain ($0.33\times0.33\times1$ mm^3 voxels, 25% gap) for cortical lesions segmentation and quantitative T2* assessment as previously detailed (Mainero et al, Brain 2015).

In all subjects, ^{11}C-PBR28 binding was assessed across brain regions (cortex, cortical lesions, white matter lesions, deep gray matter, normal appearing white matter) using standardized uptake values (SUV). To account for global signal differences across subjects, SUV maps were normalized by a pseudo-reference region (SUVR) with mean SUV in MS around the mean of SUV in HC. In 15 MS and 11 controls, we also quantified ^{11}C-PBR28 volumes of distribution (VT) using a two-tissue compartment model with a metabolite-corrected arterial plasma curve as the input function. To account for i) global signal differences across subjects and ii) inter-subject variability in the input function, VT were normalized by the same pseudo-reference region

(DVR) used for SUV. No significant differences in VT were found between MS subjects and HC in the pseudo-reference region. Statistics was performed using the R Statistics software (v2.3). Demographics and conventional MR metrics were compared in MS vs controls using Mann-Whitney-U-test. Linear regression models were used to: i) compare, in MS vs controls, SUVR and DVR across gray matter, GM, (cortical lesions, whole cortex, deep GM) and white matter, WM, (lesions and NAWM); ii) investigate in MS the relationship between SUVR and clinical (EDSS, cognitive scores), and structural MRI (cortical thickness, subcortical volume-fractions) metrics; iii) determine the relationship between SUVR and DVR. Age and TSPO affinity were included as covariates of no interest when appropriate. A correction for multiple comparisons was performed using the Holm method with a significance threshold of $p<0.05$ for each subset of analyses.

Results related to Aim1

TSPO levels in gray matter:
Relative to HC, MS cases showed increased ^{11}C-PBR28 SUVR in the whole cortex (23%) and in deep GM structures including thalamus (50%), hippocampus (28%) and basal ganglia (26%). Twenty MS subjects (SPMS=12, RRMS=8) had visible cortical lesions on 7T scans. In 2 patients no cortical lesions could be detected, while in 2 participants 7T images were discarded due to gross motion artifacts. Relative to controls' cortex, ^{11}C-PBR28 SUVR were increased by 28% in intracortical lesions and by 24% in leukocortical lesions.
The ^{11}C-PBR28 DVR were significantly increased in MS (n=15) relative to controls (n=11) in the whole cortex (30%), thalamus (44%), hippocampus (25%), and basal ganglia (19%). Cortical lesions DVR were also significantly increased (29%) relative to controls' cortex in MS patients (n=9). Due to the small number of cases with both cortical lesions and blood data, cortical lesions DVR were assessed by grouping intracortical and leukocortical lesions.

TSPO levels in white matter:
Higher TSPO levels were found in MS NAWM relative to controls WM with a 20% increase in SUVR, and a 29% increase in DVR. For WM lesions, we found a modest increase (7%) in ^{11}C-PBR28 SUVR, while higher TSPO levels could be detected in ^{11}C-PBR28 DVR (15%).

TSPO levels in RRMS and SPMS:
Corrected p-values and effect size for comparisons of ^{11}C-PBR28 SUVR and DVR in each MS subgroup relative to controls are reported in Table 1. RRMS showed significant ^{11}C-PBR28 increases in intracortical lesions and whole cortex. SUVR were also increased in thalamus, and hippocampus by ~29-22% though at an uncorrected significance level. SPMS showed significantly increased SUVR and DVR in the whole cortex (28%, 32%), cortical lesions (ranging from 24% to 36%), thalamus (64%, 58%), hippocampus (33%, 30%), and basal ganglia (34%, 25%). SUVR and DVR were increased by 27% and 32% in NAWM. Increased ^{11}C-PBR28 uptake in WM lesions was significant only for DVR (21%).

Table 1. Corrected p-values, effect size (Cohen's *d*) and standard errors for comparisons by linear regression (covarying for age and binding affinity) of ^{11}C-PBR28 uptake across different brain tissue compartments in MS subjects vs controls.

	MS vs Controls			**SPMS vs Controls**			**RRMS vs Controls**		
	p-value	***ES****	***SE***	***p-value***	***ES****	***SE***	***p-value***	***ES****	***SE***
SUVR	(n = 27 vs 14)			(n = 15 vs 14)			(n = 12 vs 14)		
Cortex	0.007	0.9	0.06	0.01	1.3	0.08	0.1	0.8	0.07
NAWM	0.02	0.9	0.07	0.01	1.3	0.08	0.5	0.5	0.07
WML	0.4	0.3	0.07	0.2	0.6	0.08	0.9	0.1	0.07
ICL	0.007	1.4	0.06	0.01	1.6	0.09	0.04	1.4	0.08
LCL	0.02	1.1	0.07	0.02	1.2	0.08	0.1	1.1	0.1
Thal	0.008	1.2	0.1	0.002	1.7	0.2	0.3	0.9	0.1
Hipp	0.006	1.3	0.06	0.003	1.6	0.09	0.1	1.1	0.07
BG	0.02	1.0	0.06	0.01	1.3	0.09	0.3	0.8	0.07
DVR	(n = 15 vs 11)			(n = 10 vs 11)			(n = 5 vs 11)		
Cortex	0.0007	1.5	0.07	0.005	1.7	0.09	0.03	1.5	0.07
NAWM	0.001	1.5	0.07	0.004	1.6	0.09	0.1	1.3	0.09
WML	0.05	0.9	0.07	0.05	1.1	0.08	1	0.3	0.06
CL[#]	0.02	1.5	0.1	0,03	3.1	0.1	0.03	1.5	0.07
Thal	0.005	1.3	0.1	0.004	1.9	0.1	0.7	0.8	0.1
Hipp	0.04	1.1	0.1	0.05	1.2	0.1	1	0.8	0.07
BG	0.02	1.1	0.07	0.02	1.4	0.07	0.9	0.5	0.06

[*] The effect size was computed by adjusting the calculation of the pooled standard deviation with weights for the sample size.
[#]SPMS, n = 6; RRMS, n = 3.
MS= multiple sclerosis; RRMS= relapsing-remitting MS; SPMS= secondary-progressive MS; normal appearing white matter (NAWM); WML= white matter lesions; ES= effect size; SE= standard error; ICL= intracortical lesions; LCL= leukocortical lesions; CL= cortical lesions; Thal= thalamus; Hipp= hippocampus; BG= basal ganglia; SUVR normalized standardized uptake values; DVR= normalized volume of distribution ratios.

Association between SUVR and DVR throughout the brain:
In all 15 MS subjects (7 with high- and 8 with mixed-affinity binding) and in 11 HC (5 with high- and 6 with mixed-affinity binding) with blood data there was a positive correlation between SUVR and DVR across all brain tissue compartments.

Association between cortical demyelination as a function of cortical depth and microglia activation:
In MS cortical demyelination, as measured by quantivative T2* (q-T2*) at 7T is accompanied by increased cortical microglia activation as measured by ^{11}C-PBR28 uptake.

Fig 1. Overlay of the general linear model significance maps (p<0.05 corrected), showing in MS subjects clusters of increased q-T2* relative to healthy controls (HC). In all of these clusters clusters ^{11}C-PBR28 SUVR were significantly higher in patients relative to HC (p<0.05 by linear regression).

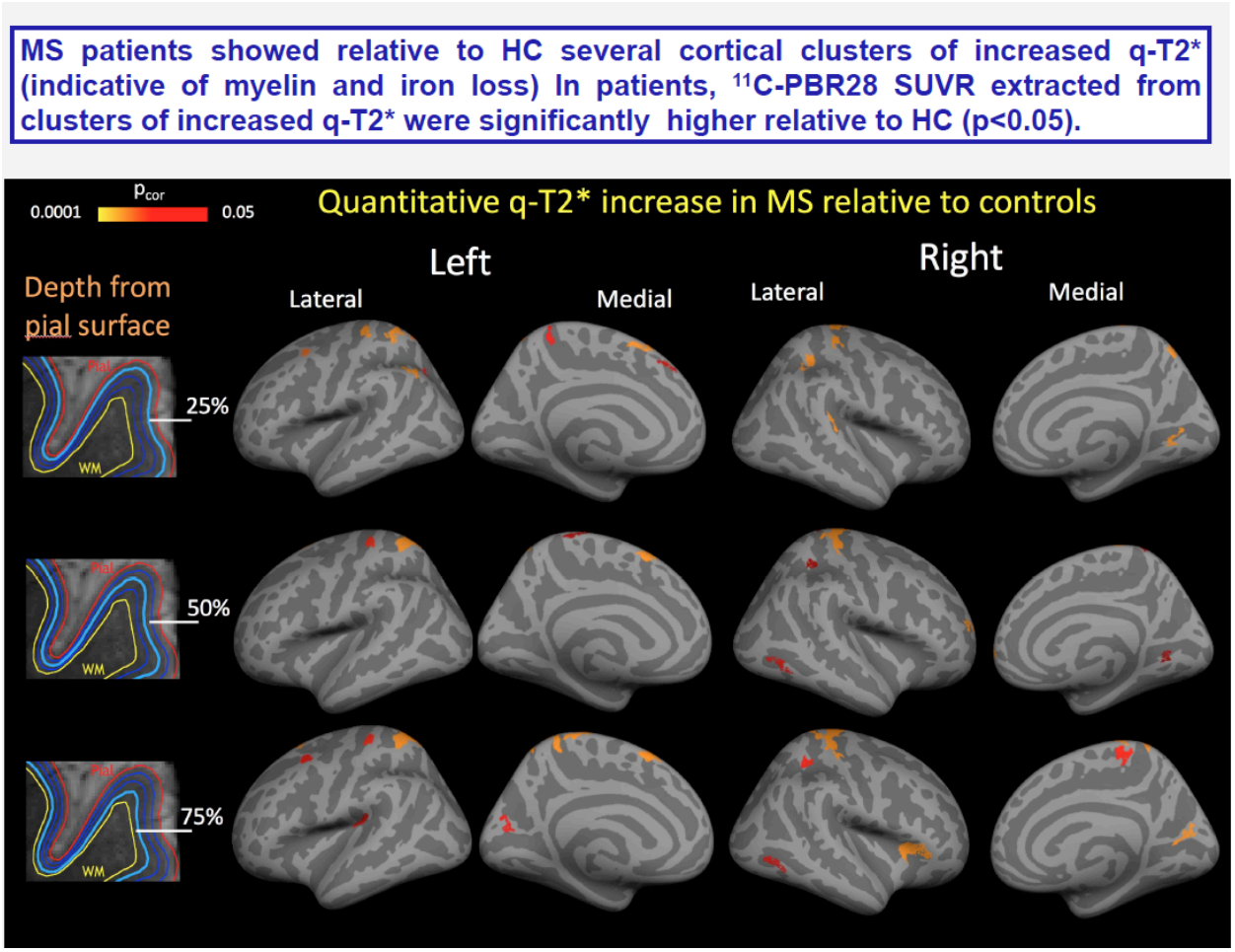

Results related to Aim2

Surface-based analysis of the association between cortical ^{11}C-PBR28 binding and clinical outcome measures:

A surface based analysis with general linear modeling was used to assess vertex-wise across the entire cortex: i) differences in ^{11}C-PBR28 SUVR between MS and HC, ii) the relationship in MS between ^{11}C-PBR28 SUVR and clinical scores (EDSS, cognitive scores). Binding affinity, age, and cortical thickness at the vertex level were used as covariates of no interest. Correction for multiple comparisons was performed using Monte-Carlo simulation with 10,000 iterations and a significance level of p<0.05. Localization of significant cortical clusters was performed using the Desikan-Killiany atlas in FreeSurfer.

The cortical surface-based analysis revealed several clusters of increased ^{11}C-PBR28 SUVR in both hemispheres in the entire MS cohort vs controls (Fig 2). The increase in ^{11}C-PBR28 cortical uptake was diffuse in SPMS, while more localized in RRMS.

Negative correlations were detected between information processing speed and memory function and ^{11}C-PBR28 uptake in widespread fronto-parietal, temporal and occipital regions, and right cingulate cortex (Fig 3).

No vertex-wise associations were found with executive function or EDSS.

Fig 2. Increased cortical ^{11}C-PBR28 uptake in SPMS and RRMS relative to controls.

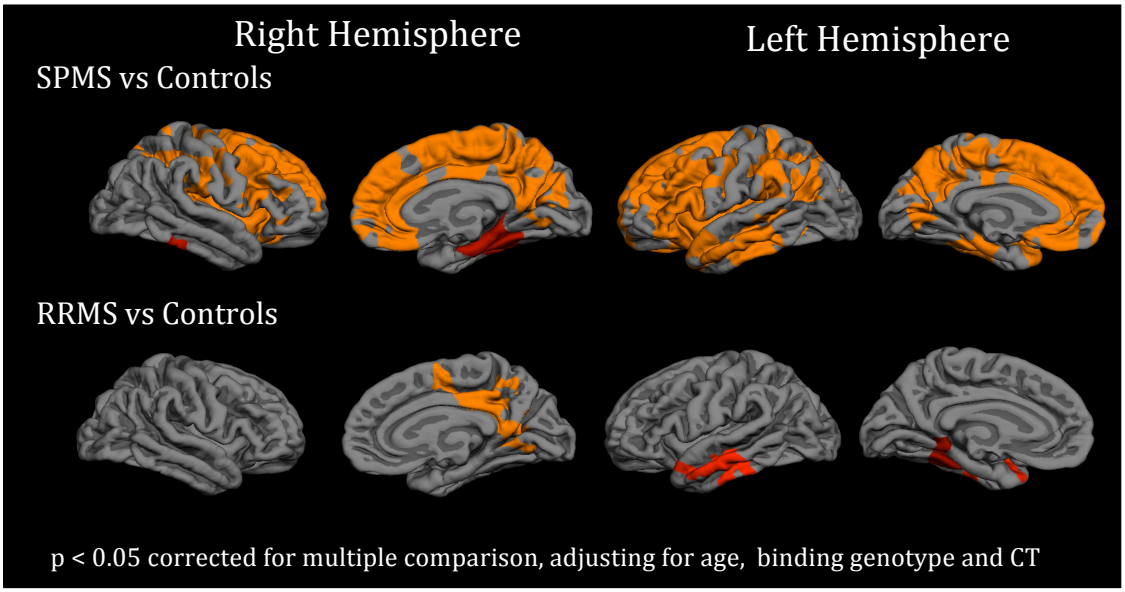

Fig 3. Cortical areas where increased ^{11}C-PBR28 cortical correlates with decreased memory and information processing speed function in MS.

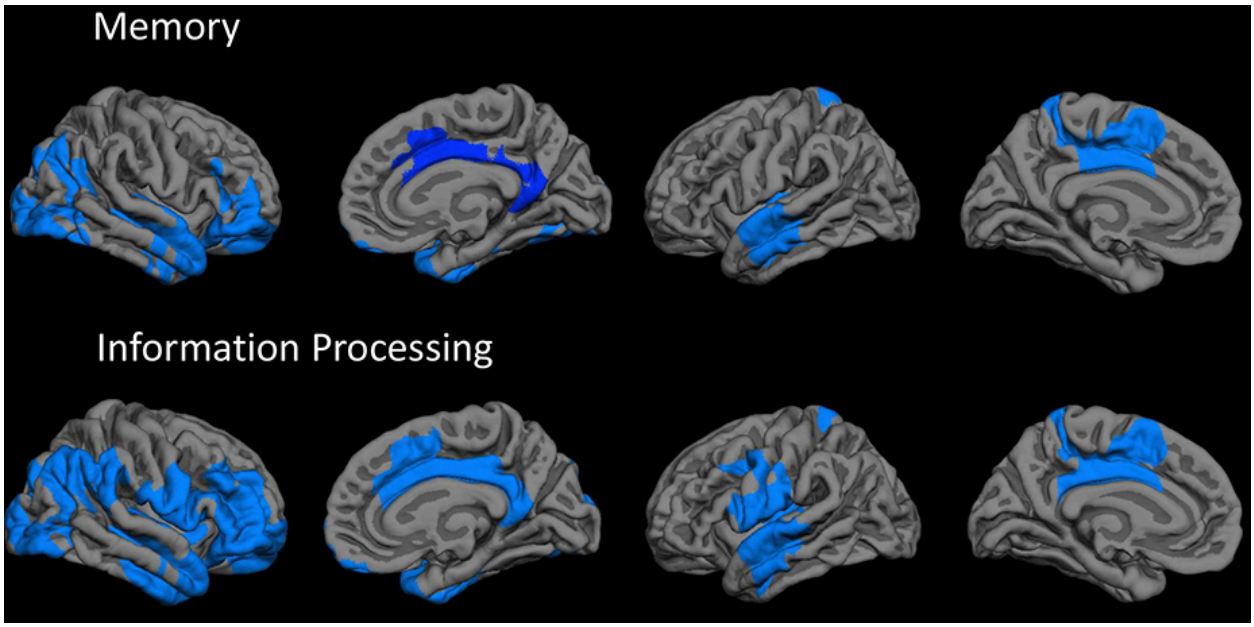

Correlation with clinical and structural MRI data

In the MS cohort, EDSS correlated positively with increased ^{11}C-PBR28 SUVR in the whole cortex, and deep GM ($p<0.05$ corrected). A positive association was also found with 11C-PBR28 uptake in the NAWM and WM lesions ($p<0.05$ corrected).

Impaired memory function scores were associated with increased TSPO levels in the thalamus. We also found that Symbol Digit Modalities Test z-scores (a measure of information processing

speed) negatively correlated with ^{11}C-PBR28 SUVR in thalamus, hippocampus and NAWM ($p<0.05$ corrected). There was no association between ^{11}C-PBR28 uptake and executive function. In all patients and in each MS subgroup, cortical thinning was associated with increased TSPO levels in the thalamus ($p<0.05$ corrected, covarying for age, binding affinity). In SPMS only, cortical thinning also correlated with neuroinflammation in the cortex and NAWM, though at an uncorrected significance level.

Conclusion

Relative to controls, MS subjects exhibited abnormally high ^{11}C-PBR28 binding across the brain, the greatest increases being in cortex and cortical lesions, deep GM, and NAWM. MS WM lesions showed relatively modest TSPO increases. With the exception of cortical lesions, where TSPO expression was similar, ^{11C}-PBR28 uptake across the brain was greater in SPMS than in RRMS.

In MS, increased ^{11}C-PBR28 binding in cortex, deep GM, and NAWM correlated with neurological disability and impaired cognitive performance; cortical demyelination correlated with increased cortical TSPO levels.

4. Impact

A) In MS, neuroinflammation is present in the cortex, cortical lesions, deep GM, and NAWM, and closely linked to poor clinical outcome and, at least partly, to neurodegeneration.

B) Distinct inflammatory-mediated factors may underlie accumulation of cortical and WM lesions.

C) Quantification of TSPO levels in MS could prove a sensitive tool for evaluating *in vivo* the inflammatory component of GM pathology, particularly in cortical lesions.

D) Microglia could constitute a potential target for monitoring disease course, especially in the compartmentalized inflammation in the cortex, and the effects of therapies.

E) Our findings could guide longitudinal evaluations in larger MS cohorts to definitely establish the role of neuroinflammation in disease pathogenesis and progression.

5. Changes/Problems

There are no changes in the SOW or study objectives.

6. Products

Proceedings from conferences:

1. Herranz E, Giannì C, Louapre C, Treaba CA, Govindarajan ST, Mangeat G, Ouellette R, Loggia M, Ward N, Klawiter EC, Sloane JA, Catana C, Hooker JM, Kinkel RP, Mainero C. The neuroinflammatory component of gray matter pathology in multiple sclerosis by in vivo combined ^{11}C-PBR28 MR-PET and 7T imaging. #4606. Proceedings of the 24th Meeting of the International Society for Magnetic Resonance in Medicine (ISMRM), Singapore, May 8-13 2016. Selected for oral presentation.

2. E. Herranz, C. Giannì, C. Louapre, C.A. Treaba, S.T. Govindarajan, R. Ouellette, G. Mangeat, M. Loggia, N. Ward, J.A. Sloane, E.C. Klawiter, C. Catana, J.M. Hooker, C. Ionete, T. Granberg, R.P. Kinkel, C. Mainero. Microglia activation is dissociated in cortex and white matter: a combined ^{11}C-PBR28 and 7T imaging study. Proceedings of the European Committee for Treatment and Research In Multiple Sclerosis Meeting (ECTRIMS), London, 2016. Selected for oral presentation.
3. E. Herranz, C. Louapre, S. Govindarajan, C.A. Treaba, C. Giannì, R. Ouellette, T. Granberg, G. Mangeat, J. Sloane, E.C. Klawiter, R.P. Kinkel, C. Mainero. Neuroinflammation and cortical demyelination in multiple sclerosis and their contribution to cognition: a ^{11}C-PBR28 MR-PET and quantitative 7T imaging study. Proceedings of the European Committee for Treatment and Research In Multiple Sclerosis Meeting (ECTRIMS), London, 2016.

Publications in peer reviewed journals:
Herranz E, Giannì C, Louapre C, Treaba CA, Govindarajan ST, Ouellette R, Loggia M, Sloane J, Madigan N, Izquierdo-Garcia D, Ward N, Mangeat G, Granberg T, Klawiter EC, Catana C, Hooker JM, Taylor N, Ionete C, Kinkel RP, **Mainero C**. The neuroinflammatory component of gray matter pathology in multiple sclerosis. Accepted for publication in the *Annals of Neurology*.

There are no inventions, patents and licenses to report.

7. Participants & Other Collaborating Organizations

Personnel	Role	Percent Effort
Caterina Mainero	Oversight responsibility for the scientific, administrative, and financial aspects of this project. Patients' screening, data collection and analysis, and supervision of post-doctoral fellows involved in these activities.	30.5 %
Elena Herranz Muelas	Post-doc, MRI and PET data acquisition and analysis, statistical analysis	50%

8. Special Reporting Requirement

Nothing to report.

9. Appendices

Copy of the abstracts presented at ISMRM and ECTRIMS.
Copy of one of the manuscripts that was listed in last year progress report but could not be submitted in the Appendices section of the report since it was still under the embargo period determined by the publisher (Louapre C, Govindarajan ST, Giannì C, Langkammer C, Sloane JA, Kinkel RP, Mainero C. Beyond focal cortical lesions in MS: an in vivo quantitative and spatial imaging study at 7 T. Neurology, 2015;85:1702–1709. PMID: 26468411.)

The neuroinflammatory component of gray matter pathology in multiple sclerosis by in vivo combined 11C-PBR28 MR-PET and 7T imaging

Elena Herranz[1,2], Costanza Giannì[1,2], Céline Louapre[1,2], Constantina Andrada Treaba[1,2], Sindhuja T Govindarajan[1], Gabriel Mangeat[1,3], Russell Ouellette[1], Marco L Loggia[1,2], Noreen Ward[1], Eric C Klawiter[1,2,4], Ciprian Catana[1,2], Jacob A Sloane[2,5], Jacob M Hooker[1,2], Revere P. Kinkel[6], and Caterina Mainero[1,2]

[1]Athinoula A. Martinos Center for Biomedical Imaging, Department of Radiology, Massachusetts General Hospital, Boston, MA, United States, [2]Harvard Medical School, Boston, MA, United States, [3]Institute of Biomedical Engineering, Polytechnique Montreal, Montreal, QC, Canada, [4]Department of Neurology, Massachusetts General Hospital, Boston, MA, United States, [5]Beth Israel Deaconess Medical Center, Boston, MA, United States, [6]University of California, San Diego, CA, United States

Synopsis

In multiple sclerosis (MS) histopathological investigations implicated neuroinflammation through microglia and/or macrophages activation in the pathogenesis of cortical and subcortical diffuse damage. By combining 11C-PBR28 positron emission tomography (PET) imaging with anatomical 7T and 3T MRI, we investigated the presence and correlates of neuroinflammation in cortex and gray matter of subjects with MS. We found that neuroinflammation was present in thalamus, hippocampus, basal ganglia as well as cortex, particularly cortical lesions, and associated with structural damage, increased neurological disability and impaired information processing speed. Our data indicate that neuroinflammation is closely associated with neurodegeneration.

Purpose

Diffuse degeneration of cortical and deep gray matter (DGM) structures is thought to play a major role in determining disease progression in multiple sclerosis (MS) [1,2]. The pathophysiological mechanisms leading to diffuse cortical and DGM degeneration in MS are still unknown. Histopathological investigations implicated neuroinflammation through microglia and/or macrophages activation in the pathogenesis of cortical and subcortical diffuse damage [3]. Activated microglia and macrophages upregulate the expression of the 18kDa translocator protein (TSPO), which can be detected in vivo by 11C-PBR28 positron emission tomography (PET) imaging [4]. Here, in a heterogenous MS cohort, we combined 11C-PBR28 imaging on a high resolution, integrated human MR-PET system with ultra high resolution 7 Tesla (7T) MRI to i) investigate the presence of activated microglia and macrophages throughout the cortex and DGM, ii) assess their relation with neurodegeneration, iii) and with measures of neurological disability (Expanded Disability Status Scale, EDSS) and information processing speed (Symbol Digit Modalities Test, SDMT) frequently affected in MS.

Methods

Eighteen MS subjects (11 secondary progressive, SP, and 7 relapsing remitting, RR; mean±SD age=49±11 years; median, range EDSS=6.5, 2-7.5) and 12 age- and TSPO affinity binding (as assessed by the Ala147Thr TSPO polymorphism [5]) matched healthy controls (HC) underwent 90-minutes of 11C-PBR28 MR-PET (Siemens BrainPET). Anatomical 3T MR scans were simultaneously acquired for: a) cortical surface reconstruction, cortical thickness (CT) measurement, using FreeSurfer b) DGM segmentation (thalamus, hippocampus and basal ganglia), volume estimation, using FIRST-FSL c) MR-PET image registration (Figure1). Standardized uptake value (SUV) maps were created for 60-90-minute PET frame (1.25 mm isotropic voxels) and normalized (SUVR), to take into account global differences across subjects, to a pseudo-reference region with SUV levels similar in HC and MS. Seventeen patients underwent 7T (Siemens, 32-channel head coil) acquisitions of T2* gradient-echo sequences (0.33x0.33x1mm3) to segment intra-cortical (IC) and leukocortical (LC) lesions (Figure1). Five patients, however, were excluded due to motion artifacts, 4 patients had no cortical lesions (CL). Lesional, whole cortex and DGM masks were co-registered to 11C-PBR28 maps to extract SUVRs. In HC, SUVRs were obtained from cortex and DGM. Linear regression models were used to compare, in MS vs HC, SUVRs across GM (CL, whole cortex, DGM), as well as CT and DGM volumes, and to assess in MS the relationship between SUVRs, CT, DGM atrophy, and clinical metrics (EDSS, SDMT). Age, gender, TSPO affinity and intracranial volume were included as regressors when appropriate with a significant threshold of $p<0.05$ (we denote as p^*, the p-value corrected for multiple comparisons and as p the uncorrected p-value). Using Freesurfer, a general linear model (GLM) was run on a vertex-by-vertex basis across the whole cortex ($p^*<0.05$, corrected for multiple comparisons) to assess: i) differences in 11C-PBR28 SUVRs in MS vs HC ii) the relationship in MS between 11C-PBR28 SUVRs and clinical scores. Prior to GLM statistics, each individual SUVR map was coregistered to cortical surfaces, sampled at mid-cortical distance, smoothed along the surface with a 10 mm full-width at half maximum Gaussian kernel, and normalized to a common template surface. TSPO affinity and CT at the vertex level were used as nuisance factors.

Results

Relative to controls, MS subjects had increased 11C-PBR28 SUVRs in thalamus (~50%, $p^*=0.01$), hippocampus (~40%, $p^*=0.002$), basal ganglia (22%, $p^*=0.01$). Increased 11C-PBR28 uptake was also observed in whole cortex (~18%, $p^*=0.01$), and even more in CL (~36%, $p^*=0.01$), with similar SUVRs between LCL and ICL (Figure2). Patients had decreased mean CT (MS=(2.3±0.1)mm, HC=(2.3±0.1) mm, p=0.05) and thalamic volume (MS=(8252±2280)mm3, HC=(9574±1284)mm3, p=0.006) than HC. Cortical thinning correlated with higher SUVRs in thalamus (p=0.02), hippocampus (p=0.03) and cortex (p=0.03). The cortical surface-based analysis disclosed a cluster of increased 11C-PBR28 uptake in MS vs HC in the middle temporal cortex of the right hemisphere, extending to the inferior temporal cortex (Figure3). Negative correlations were detected between SDMT scores and 11C-PBR28 uptake in the superior frontal and middle temporal cortex of both hemispheres,in the right transverse temporal and frontal cortex, and left lateral occipital and precentral cortex (Table 1, Figure3). Impaired SDMT scores were also associated with subcortical GM glial activationin thalamus (p=0.03) and hippocampus (p=0.02) Neurological disability (EDSS) correlated with increased11C-PBR28uptake in thalamus (p=0.02), basal ganglia (p=0.04), and whole cortex (p=0.05), though no regional cortical associations were found at the vertex-wise GLM analysis.

Conclusion

Our data indicate that neuroinflammation in MS, likely mediated by activated microglia, is a diffuse process throughout cortex, particularly cortical lesions, and DGM and it is closely linked to neurodegeneration and poor clinical outcome.

Acknowledgements

Acknowledgments: This study was supported by Clafin Award; NMSS RG 4729A2/1, US Army W81XWH-13-1-0112

References

1. Kutzelnigg A, Lucchinetti CF, Stadelmann C, et al. Cortical demyelination and diffuse white matter injury in multiple sclerosis. Brain. 2005; 128: 2705-12.

2. Kutzelnigg A, Lassmann H, et al. Cortical demyelination and diffuse in multiple sclerosis: a susbstrate for cognitive deficits?. J Neurol Sci. 2006; 245:123-6.

3. Lassmann H, Mechanism of inflammation induced tissue injury in multiple sclerosis. 2008 J. Neurol.Sci. 274:45-4.

4. Brown AK, Fujita M, Fujimura Y et al. Radiation dosimetry and biodistribution in monkey and man of 11C-PBR28: a PET radioligand to image inflammation. J Nucl Med.2007; 48: 2072-2079

5. Owen DR, Gunn RN, Rabiner EA et al. Mixed-affinity binding in humans with 18-kDa translocator protein ligands.JNuclMed. 2011; 52:24-32

Abstract ID: 4606

Figures

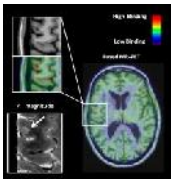

Figure 1. Increased 11C-PBR28 uptake topographically associated with the presence of a leukocortical lesion on the 3T image and on the co-registered 7T T2* image of a 40 years old female, SPMS patient.

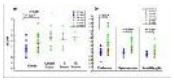

Figure 2. Mean SUVR values in controls (HC) and patients (MS). a) Whole cortex and cortical lesions and b) DGM; Bars indicate group averages for HAB=High Affinity Binder, MAB=Mixed Affinity Binder. (*) $P < 0.05$, by linear regression and corrected for multiple comparison.

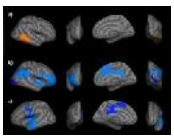

Figure 3. FreeSurfer surface-based analysis of 11C-PBR28 uptake. a) Regions where SUVR was increased ($p^*<0.05$, corrected) in subjects with MS compared to HC, correcting for age and PBR affinity (Right Hemisphere). (b-c) Regions where 11C-PBR28 uptake correlates negatively ($p<0.05$, corrected) with SDMT scores.Right hemisphere (b) and left hemisphere (c).

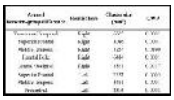

TABLE 1. Correlation between cortical 11C-PBR28 SUVR uptake and SDMT: Regions where cortical 11C-PBR28 SUVR uptake in patients with MS correlated negatively with SDMT scores on surface-based analysis. CWP = cluster-wise probability.

Abstract Preview - Step 3/4

- print version -

Topic: Pathology and pathogenesis of MS - Imaging

Title: Microglia activation is dissociated in cortex and white matter: a combined ^{11}C-PBR28 and 7T imaging study

Author(s): *E. Herranz[1], C. Giannì[1], C. Louapre[1], C.A. Treaba[1], S.T. Govindarajan[2], R. Ouellette[2], G. Mangeat[2,3], M. Loggia[1], N. Ward[2], J.A. Sloane[4,5], E.C. Klawiter[1], C. Catana[1], J.M. Hooker[1], C. Ionete[6], T. Granberg[1,7], R.P. Kinkel[8], C. Mainero[1]*

Institute(s): [1]Massachusetts General Hospital, Harvard Medical School, [2]Massachusetts General Hospital, Boston, MA, United States, [3]Institute of Biomedical Engineering, Polytechnique Montreal, Montreal, QC, Canada, [4]Beth Israel Deaconess Medical Center, [5]Harvard Medical School, [6]UMass Memorial Medical Center, Boston, MA, United States, [7]Intervention and Technology, Karolinska Institute, Stockholm, Sweden, [8]University of California San Diego, San Diego, CA, United States

Text: **Background:** Neuropathological studies of multiple sclerosis (MS) suggest that microglia activation plays a key role in cortical lesions (CL) pathogenesis, and that the innate immune system-mediated inflammatory events underlying the development of MS pathology are dissociated in cortex and white matter (WM).
Goals: To investigate, using 7T MRI and magnetic resonance-positron emission tomography (MR-PET) imaging with ^{11}C-PBR28, the *in vivo* pathological and clinical relevance of microglia activation in lesioned and non-lesioned tissue in cortex and WM in secondary-progressive and relapsing-remitting MS (SPMS, RRMS).
Methods: Thirteen SPMS and 9 RRMS patients, and 14 age- and translocator protein (TSPO) affinity matched healthy controls (HC) underwent ^{11}C-PBR28 MR-PET imaging. Anatomical MR scans were acquired for FreeSurfer reconstruction. ^{11}C-PBR28 binding was measured in all cases using normalized 60-90 minutes standardized uptake values (SUVR), in 14 MS and 11 HC also with volume of distribution ratios (V_TR). MS WM and cortical lesions (CL, in 12 MS) were segmented on 7T T_2* scans. ^{11}C-PBR28 SUVR and V_TR were extracted in lesions, whole cortex, normal-appearing WM (NAWM). MS cognitive function was assessed using a modified version of the Minimal Assessment of Cognitive Function in MS and by averaging z-scores from individual tests. Linear regression was used to compare ^{11}C-PBR28 uptake between groups, and assess the relation with clinical metrics. Age, gender, TSPO affinity were included as regressors.
Results: Relative to HC, all MS exhibited abnormally increased ^{11}C-PBR28 SUVR in CL (SUVR: 27%, p=0.001), whole cortex (SUVR: 22%, p=0.002; V_TR: 31%, p=0.0001), and NAWM (22%, p=0.008; V_TR: 29%, p=0.008). ^{11}C-PBR28 uptake in MS WM lesions was modestly increased vs HC (SUVR: 10%; V_TR: 17%, p=0.06). Twenty-seven CL were identified in RRMS, 223 in SPMS with a ~21% (p=0.01) and a ~32% (p=0.007) increase in SUVR, respectively, relative to HC cortex. Microglia activation, relative to HC, was greater in SPMS than in RRMS in NAWM (p=0.004). Reduced cognitive function correlated with increased SUVR in NAWM (p=0.02) and CL (p=0.05). Worsening of EDSS was related to increased NAWM PBR uptake (p=0.04).
Conclusions: Distinct microglia-mediated events may underlie cortical and WM pathology. Quantification of microglia activation is a sensitive tool for evaluating in vivo the inflammatory component of cortical pathology at all disease stages.
Disclosure: This study was supported partly by the Clafin Award; partly by a grant from the National MS Society (NMSS) RG 4729A2/1, and partly by the Department of Defense (DoD) US Army W81XWH-13-1-0112 Award.
EH, GM, ML, CAT, STG, NW, JAS, RO, CC, JMH,TG: no disclosure
Dr Mainero has received research support from EMD Merck Serono and speaker fees from Biogen
Dr Giannì has received a fellowship from FISM 2012/B/4
Dr Louapre received a fellowship from ARSEP foundation
Dr Klawiter has received consulting fees from Biogen Idec and Mallinckrodt Pharmaceuticals and research funding from Roche and Atlas5d
Dr. Kinkel reports personal fees from Genzyme ; A Sanofi Corp, personal fees from Biogen Idec, grants from Acclerated Cure Project, personal fees from Novartis, outside the submitted work

Travel Grant / Young Scientific Investigator's Sessions: I will not apply for Travel Grant or Young Scientific Investigator's Sessions

Preferred Presentation Type: Oral or poster presentation

Conference: 32nd Congress of the European Committee for Treatment and Research in Multiple Sclerosis · Abstract: A-777-0023-02043 · **Status: Submitted**

Print Back

Abstract Preview - Step 3/4

- print version -

Topic: Pathology and pathogenesis of MS - Imaging

Title: Neuroinflammation and cortical demyelination in multiple sclerosis and their contribution to cognition: a ^{11}C-PBR28 MR-PET and quantitative 7T imaging study.

Author(s): *E. Herranz[1], C. Louapre[1], S. Govindarajan[2], C.A. Treaba[1], C. Giannì[1], R. Ouellette[2], T. Granberg[1,3], G. Mangeat[2,4], J. Sloane[5], E.C. Klawiter[1], R.P. Kinkel[6], C. Mainero[1]*

Institute(s): [1]Massachusetts General Hospital, Harvard Medical School, [2]Massachusetts General Hospital, Boston, MA, United States, [3]Intervention and Technology, Karolinska Institute, Stockholm, Sweden, [4]Institute of Biomedical Engineering, Polytechnique Montreal, Montreal, QC, Canada, [5]Beth Israel Deaconess Medical Center, Harvard Medical School, Boston, MA, [6]University of California San Diego, San Diego, CA, United States

Text: **Background**: Cortical demyelination contributes to cognitive decline in multiple sclerosis (MS), but the underlying pathophysiological mechanisms are still unknown. Histopathological examinations suggested that cortical demyelination in MS might develop following meningeal inflammation accompanied by cortical microglia activation.

Aim: To assess, using quantitative T2* (q-T2*) at 7T and ^{11}C-PBR28 MR-PET: 1) whether MS cortical demyelination is characterized by the presence of microglial pathology 2) the relative contribution of cortical demyelination and cortical microglia activation to decreased information processing speed.

Methods: Sixteen MS patients (mean age: 50 ± 10 years) and 12 age- and translocator protein affinity binding matched healthy controls (HC) underwent ^{11}C-PBR28 MR-PET. Anatomical MR scans were acquired for FreeSurfer cortical surface reconstruction. Normalized 60-90 minute standardized uptake value (SUVR) maps (1.25 mm isotropic voxels) were registered to cortical surfaces and sampled at 50% depth from the pial surface. Subjects also underwent multi-echo T2* imaging at 7T (0.33x0.33x1 mm^3) for intracortical laminar assessment of q-T2* at 25%, 50% and 75% depth from the pial surface. A general linear model was used to assess vertex-wise in the cortex i) differences between MS and HC in q-T2* at each cortical depth ii) the relationship, in MS, between Symbol Digit Modalities Test (SDMT) and cortical q-T2* at all 3 depths and ^{11}C-PBR28 at 50% depth. Finally, in clusters showing significant q-T2* differences in MS vs HC, the corresponding ^{11}C-PBR28 SUVR were extracted and compared between the groups using multi-linear regression. Age and PBR affinity were included as nuisance regressors ($p < 0.05$ corrected for multiple comparison).

Results: MS patients showed relative to HC several cortical clusters of increased q-T2* (indicative of myelin and iron loss) in juxtameningeal cortical layers (25% depth) and deeper cortical laminae (50%, 75% depth). Clusters with increased q-T2* in patients also had significantly higher ^{11}C-PBR28 SUVR relative to HC ($p < 0.05$). In patients, increase in cortical q-T2* at 25%, 50% and 75% depth and in cortical ^{11}C-PBR28 SUVR at 50% depth negatively correlated with SDMT scores in widespread frontal, parietal, temporal and occipital regions.

Conclusions: MS cortical demyelination is accompanied by increased microglia activation. Both pathological processes contribute to decreased information processing speed.

Disclosure: This study was supported partly by the Clafin Award; partly by a grant from the National MS Society (NMSS) RG 4729A2/1, and partly by the Department of Defense (DoD) US Army W81XWH-13-1-0112 Award.

EH, GM, CAT, STG, JAS, RO, TG,: no disclosure

Dr Mainero has received research support from EMD Merck Serono and speaker fees from Biogen.

Dr Giannì has received a fellowship from FISM 2012/B/4

Dr Louapre received a fellowship from ARSEP foundation

Dr Klawiter has received consulting fees from Biogen Idec and Mallinckrodt Pharmaceuticals and research funding from Roche and Atlas5d

Dr. Kinkel reports personal fees from Genzyme ; A Sanofi Corp, personal fees from Biogen Idec, grants from Acclerated Cure Project, personal fees from Novartis, outside the submitted work

Travel Grant / Young Scientific Investigator's Sessions: I will not apply for Travel Grant or Young Scientific Investigator's Sessions

Preferred Presentation Type: Oral or poster presentation

Conference: 32nd Congress of the European Committee for Treatment and Research in Multiple Sclerosis · Abstract: A-777-0023-02177 · **Status: Submitted**

Print Back

Beyond focal cortical lesions in MS

An in vivo quantitative and spatial imaging study at 7T

Céline Louapre, MD, PhD
Sindhuja T. Govindarajan, MS
Costanza Giannì, MD
Christian Langkammer, PhD
Jacob A. Sloane, MD, PhD
Revere P. Kinkel, MD
Caterina Mainero, MD, PhD

Correspondence to Dr. Mainero: caterina@nmr.mgh.harvard.edu

ABSTRACT

Objectives: Using quantitative T2* 7-tesla (7T) MRI as a marker of demyelination and iron loss, we investigated, in patients with relapsing-remitting multiple sclerosis (RRMS) and secondary progressive multiple sclerosis (SPMS), spatial and tissue intrinsic characteristics of cortical lesion(s) (CL) types, and structural integrity of perilesional normal-appearing cortical gray matter (NACGM) as a function of distance from lesions.

Methods: Patients with MS (18 RRMS, 11 SPMS), showing at least 2 CL, underwent 7T T2* imaging to obtain (1) magnitude images for segmenting focal intracortical lesion(s) (ICL) and leukocortical lesion(s) (LCL), and (2) cortical T2* maps. Anatomical scans were collected at 3T for cortical surface reconstruction using FreeSurfer. Seventeen age-matched healthy participants served as controls.

Results: ICL were predominantly located in sulci of frontal, parietal, and cingulate cortex; LCL distribution was more random. In MS, T2* was higher in both ICL and LCL, indicating myelin and iron loss, than in NACGM ($p < 0.00003$) irrespective of CL subtype and MS phenotype. T2* was increased in perilesional cortex, tapering away from CL toward NACGM, the wider changes being for LCL in SPMS. NACGM T2* was higher in SPMS relative to RRMS ($p = 0.006$) and healthy cortex ($p = 0.02$).

Conclusions: CL had the same degree of demyelination and iron loss regardless of lesion subtype and disease stage. Cortical damage expanded beyond visible CL, close to lesions in RRMS, and more diffusely in SPMS. Evaluation of NACGM integrity, beyond focal CL, could represent a surrogate marker of MS progression. *Neurology*® 2015;85:1702–1709

GLOSSARY

CL = cortical lesion(s); **DIR** = double inversion recovery; **EDSS** = Expanded Disability Status Scale; **FLASH** = fast low-angle shot; **GM** = gray matter; **GRE** = gradient echo; **ICL** = intracortical lesion(s); **LCL** = leukocortical lesion(s); **MEMPR** = magnetization-prepared rapid acquisition with multiple gradient echoes; **MS** = multiple sclerosis; **NACGM** = normal-appearing cortical gray matter; **NAWM** = normal-appearing white matter; **RRMS** = relapsing-remitting multiple sclerosis; **SPMS** = secondary progressive multiple sclerosis; **TA** = acquisition time; **TE** = echo time; **TR** = repetition time; **WM** = white matter.

Demyelinating cortical lesion(s) (CL) are thought to contribute to disease progression in multiple sclerosis (MS).[1–3] Seven-tesla (T) T2* gradient-echo imaging has shown increased sensitivity (approximately 50%–90%) to detect MS CL.[4–6] Ex vivo MRI studies demonstrated increased T2* in MS CL, pathologically related to demyelination and iron loss.[5,6] Histopathologic–MRI correlations suggested that MRI-visible CL may represent the tip of the iceberg[7] underlying a more diffuse demyelinating cortical process.

We previously demonstrated in vivo T2* increase at different depths of the cortical width throughout stages of MS, associated with worsening disability.[8] Quantitative T2* changes were not confined to focal CL but were also found globally in the normal-appearing cortical gray matter (NACGM) in secondary progressive MS (SPMS). The relationship between pathology in NACGM and in focal CL at different MS stages is unclear: NACGM abnormalities could either reflect a diffuse degenerative process or abnormalities in normal cortex surrounding CL. Because CL may underlie different pathologic processes including endogenous remyelination

Supplemental data at Neurology.org

From the Athinoula A. Martinos Center for Biomedical Imaging (C. Louapre, S.T.G., C.G., C. Langkammer, C.M.), Charlestown, MA; Harvard Medical School (C. Louapre, C.G., C. Langkammer, C.M.), Boston, MA; Beth Israel Deaconness Medical Center (J.A.S.), Boston, MA; and Department of Neurosciences (R.P.K.), University of California San Diego, CA.

Go to Neurology.org for full disclosures. Funding information and disclosures deemed relevant by the authors, if any, are provided at the end of the article.

depending on their location across the cortical/subcortical width,[9] their extent on surrounding NACGM may vary according to CL subtype.

In a heterogeneous MS cohort, we used 7T quantitative T2* MRI to (1) map the spatial distribution and frequency of CL subtypes, (2) assess whether the degree of tissue pathology within CL varies depending on disease stage, and (3) quantify perilesional pathology in CL subtypes as a function of distance from lesions. We hypothesized that patients with SPMS had more severe pathology within focal CL and perilesional cortex.

METHODS

Standard protocol approvals, registrations, and patient consents. The institutional review board of our institution approved all study procedures, and participants provided written informed consent to participate in the study.

Participants. Twenty-nine patients (20 women; mean age 44.1 years ±9.2 SD) with a diagnosis of MS[10] and who displayed at least 2 focal intracortical lesion(s) (ICL) or leukocortical lesion(s) (LCL) on 7T scans were retrospectively selected from a cohort of 41 patients with MS participating in a prospective study assessing cortical pathology at 7T.[8] ICL included lesions originating from the pial surface and extending at different depths throughout the cortical width (type III–IV lesions), and type II lesions[8,11]; LCL were defined as extending through gray matter (GM)/white matter (WM) without reaching the pial surface. Seventeen age-matched healthy individuals (9 women, mean age 39.3 years ±8.8 SD) served as controls.

Clinical course of patients included RRMS (n = 18) and SPMS (n = 11). Twenty-two of 29 patients were receiving stable treatment (at least 6 months) with disease-modifying therapies (interferon beta or glatiramer acetate: 6 RRMS, 5 SPMS; BG-12: 1 RRMS; natalizumab: 6 RRMS, 3 SPMS; rituximab: 1 SPMS). Neurologic disability was assessed using the Expanded Disability Status Scale (EDSS)[12] within a week from MRI scans. Disease severity was evaluated using the Multiple Sclerosis Severity Score.[13]

General exclusion criteria included significant psychiatric and/or neurologic disease (other than MS for patients), major medical comorbidity, pregnancy, and contraindications for MRI.

MRI data acquisition. All study participants underwent 2 imaging sessions at 7T and 3T (Siemens scanners) using 32-channel coils. The 7T protocol included acquisition of (1) multiecho 2-dimensional (2D) fast low-angle shot (FLASH) T2*-weighted spoiled gradient-echo (GRE) images with repetition time (TR) = 2,210 milliseconds (ms), echo time (TE) = 6.44 + 3.32n [n = 0, …, 11] ms, flip angle = 55°, 2 slabs of 40 slices each to cover the supratentorial brain, resolution = 0.33 × 0.33 × 1 mm^3 (25% gap), and acquisition time (TA) for each slab = approximately 10 minutes; (2) a T1-weighted 3D magnetization-prepared rapid acquisition gradient echo sequence (TR/inversion time/TE = 2,600/1,100/3.26 ms, flip angle = 9°, resolution = 0.60 × 0.60 × 1.5 mm^3, TA = 5.5 minutes) for coregistration of 7T GRE data with cortical surfaces; and (3) a single-echo 2D FLASH T2*-weighted spoiled GRE pulse sequence (TR/TE = 1,700/21.8 ms; the other parameters were identical to the multiecho 2D FLASH T2* sequence).

During the 3T session, a structural scan with a 3D magnetization-prepared rapid acquisition with multiple gradient echoes (MEMPR) (TR/inversion time = 2,530/1,200 ms, TE = 1.7, 3.6, 5.4, 7.3 ms, resolution = 0.9 × 0.9 × 0.9 mm^3, TA = approximately 6.5 minutes) was obtained for cortical surface reconstruction and coregistration with 7T data.

MRI data processing. ***WM lesion volume.*** WM lesions were segmented on magnitude images from 7T single-echo FLASH T2* scans with a semiautomated method implemented in 3D Slicer version 4.2.0 (http://www.slicer.org). WM lesion volume was computed using fslstats, part of FSL (FMRIB Software Library, http://fsl.fmrib.ox.ac.uk/fsl/fslwiki/FSL).

Cortical surface reconstruction. Reconstruction of pial and WM surfaces was performed using the software FreeSurfer, version 5.3.0 (http://surfer.nmr.mgh.harvard.edu/), according to a multistep procedure that calculates the GM/WM border and the CSF/GM (pial) border in the 3D MEMPR volume,[14] currently the recommended anatomical sequence for FreeSurfer pipeline.[15] Topologic defects in cortical surfaces due to WM and LCL were corrected using a semiautomated procedure with lesions filling.

Mean cortical thickness (mm) was measured in each participant as previously described[15] and used as covariate of no interest in statistical analyses.

Quantitative T2* maps. Quantitative T2* maps were generated from 7T multiecho T2* scans in each participant as previously described.[8,16,17] Briefly, T2* signal, corrected for susceptibility-induced through-slice dephasing, was fitted vs TE voxel-wise using a Levenberg–Marquardt nonlinear regression model. R^2 goodness of fit was measured, and voxels with poor goodness of fit ($R^2 < 0.8$) were excluded from further analyses. T2* maps were registered onto the corresponding 3T cortical surfaces using a 2-step procedure, as previously described.[16,17] The registered data were then concatenated into a whole brain volume using FreeSurfer tools and resampled at 0.33 × 0.33 × 0.33 mm^3 isotropic voxels.

Cortical lesion segmentation, count, and volume. Focal ICL and LCL that appeared as focal cortical hyperintensities and extended for at least 3 voxels and across 2 consecutive slices on magnitude images from 7T single-echo FLASH T2* were segmented by consensus by 2 experienced raters (C.M., C. Louapre) using Slicer.

In each participant, single-echo T2* images, ICL, LCL, and NACGM masks were registered onto the corresponding 3T cortical surfaces using a 2-step procedure based on boundary-based registration[18] as previously described.[16,17] ICL and LCL count and volume were computed using FreeSurfer and FSL tools (mri_volcluster and fslstats, respectively).

Cortical lesion spatial analysis and probability distribution map. Using FreeSurfer tools, individual ICL and LCL masks were projected on each participant's cortical surface resulting in 2D lesional masks. Using the cortex curvature map, we then quantified the total area of cortical lesions belonging to sulci (displaying positive curvature values) and to gyri (displaying negative curvature values).

Subsequently, 2D cortical lesion masks were normalized to a common surface template, "fsaverage," using FreeSurfer. Lesion probability maps were then generated by averaging individual ICL and LCL normalized masks. Peaks of lesion probability were localized using the Desikan atlas in FreeSurfer.

Quantitative T2* analysis of lesional, perilesional, and normal-appearing cortex. In each participant, we computed mean T2* (ms) in ICL, LCL, and NACGM masks previously coregistered to the corresponding cortical surfaces. Given that the focus of the study was the cortex, for LCL, T2* was measured

only in the intracortical portion of the mask (i.e., the intersection between the LCL mask and the FreeSurfer cortical ribbon mask).

We further analyzed the extent of ICL and LCL pathology toward perilesional cortex. Because of the thin and circumvolved geometry of the cortex, the analysis was performed on individual 2D ICL and LCL masks. T2* relaxation time was then mapped at 50% depth from the pial surface and computed as a function of distance from the ICL, and mapped at 75% depth from the pial surface and computed as a function of distance from the LCL; 0% depth was the pial surface and 100% depth was the WM/GM boundary.

Each vertex on the participant's cortical surface was assigned its geodesic distance from the lesions, the geodesic distance being the number of edges in the shortest path connecting a given vertex to a lesion (figure e-1 on the *Neurology*® Web site at Neurology.org). For each participant, we calculated T2*(N), the average of T2* values over all vertices being at a given geodesic distance N of the lesions. As previously observed,[16,17] T2* values varied across the cortex, and accordingly, T2* within lesions is dependent on lesion location in individual participants. Therefore, to analyze T2* decay surrounding lesions across the whole MS group, we subtracted T2*(N) by its baseline value defined as the minimum over a range of $10 < N < 20$.

Statistics. Demographic and/or imaging metrics were compared between patients and controls, and between RRMS and SPMS using a Mann–Whitney *U* test or Student *t* test as appropriate and a χ^2 test for sex repartition.

In the whole MS group, each patient's ratio of ICL and LCL area in sulci relative to the total lesional area was compared to its ratio of sulci surface relative to the total cortical surface using a paired *t* test.

Mean T2* in NACGM in each MS group and cortical T2* in controls were compared by linear regression using age and cortical thickness as nuisance factors. Mean T2* in each lesion mask was compared with NACGM T2* in each patient group by paired *t* test, and with cortical T2* in controls by linear regression using age and mean cortical thickness as nuisance factors.

Finally, we determined the geodesic distance up to which T2*(N) was significantly different from distant NACGM (N = 20) using paired *t* test.

All statistical analyses were performed with R software (version 2.13.1), and *p* values <0.05 were considered statistically significant. A false discovery rate method was applied to correct for multiple comparisons when comparing different cortical tissue compartments within and across groups.

RESULTS

Demographics. Participants' demographic, clinical, and MRI variables are reported in table 1. Disease duration, EDSS scores, and WM lesion volume were higher in SPMS relative to RRMS ($p < 0.005$). Age at disease onset tended to be younger in SPMS than in RRMS ($p = 0.06$). ICL count, ICL volume, and LCL volume were also higher in SPMS relative to RRMS ($p < 0.05$).

Spatial distribution of focal cortical lesions. In the entire MS cohort, the highest distribution of ICL was in superior, middle frontal areas and central sulcus, followed by parietal, cingulate, and temporal cortex (table 2, figure 1). LCL distribution was more random. There were fewer ICL in RRMS than in SPMS and they were mainly distributed in the central sulcus, frontal areas, and cingulate cortex (figure e-2).

In each patient, both ICL and LCL were predominantly identified in cortical sulci, with an average 84% of ICL area and 64% of LCL area in sulci in

Table 1 Demographic, clinical, and MRI characteristics of participants

	Controls	MS	RRMS	SPMS
No.	17	29	18	11
Sex, M/F	8/9	9/20	4/14	5/6
Age, y	39.3 (8.8) [28–56]	44.1 (9.2) [26–61]	43.1 (9.5) [26–57]	45.7 (8.8) [27–61]
Age at onset, y	—	32.6 (9)	35.1 (8.9)	28.5 (7.8)
Disease duration, y	—	11.5 (7.1) [2–28]	8.0 (4.5) [2–16]	17.2 (7) [7–28][a]
EDSS score	—	3 (1–7)	2.5 (1–6)	4 (3–7)[a]
MSSS	—	3.81 (0.94–7.97)	3.57 (0.94–7.97)	4.94 (2.34–7.97)
WMLV, mm^3	—	6,607 (9,653)	2,732 (2,327)	12,949 (13,433)[a]
Total CL count	—	23 (5–188)	10 (5–36)	61 (6–188)[a]
Total CL volume		2,245 (3,047)	763 (796)	4,671 (3,807)[a]
ICL count	—	9 (0–55)	6 (0–23)	30 (2–55)[b]
ICL volume, mm^3	—	1,224 (2,552)	393 (449)	2,585 (3,823)[b]
LCL count	—	6 (0–137)	3.5 (0–18)	37 (0–137)[b]
LCL volume, mm^3	—	1,020 (1,700)	370 (508)	2,085 (2,376)

Abbreviations: CL = cortical lesion(s); EDSS = Expanded Disability Status Scale; ICL = intracortical lesion(s); LCL = leukocortical lesion(s); MS = multiple sclerosis; MSSS = Multiple Sclerosis Severity Score; RRMS = relapsing-remitting multiple sclerosis; SPMS = secondary progressive multiple sclerosis; WMLV = white matter lesion volume.
Results are expressed as mean (SD) [range], except for EDSS, MSSS, and lesion count, which are expressed as median (range). The *p* values are corrected for multiple comparisons using false discovery rate.
[a] $p < 0.005$, RRMS vs SPMS.
[b] $p < 0.05$, RRMS vs SPMS.

Table 2 Location of clusters exhibiting the highest spatial distribution for ICL and LCL in the entire MS group

ICL		LCL	
Location	**Frequency, %**	**Location**	**Frequency, %**
Left hemisphere			
Superior frontal	10.3	Superior frontal	6.9
Caudal middle frontal	6.9	Rostral middle frontal	6.9
Precentral	13.8	Supramarginal	6.9
Postcentral	10.3	Superior parietal	6.9
Paracentral	6.9		
Supramarginal	10.3		
Inferior parietal	6.9		
Superior parietal	6.9		
Superior temporal	6.9		
Precuneus	6.9		
Isthmus cingulate	6.9		
Pericalcarine	6.9		
Right hemisphere			
Superior frontal	10.3	Superior frontal	10.3
Caudal middle frontal	10.3	Caudal middle frontal	6.9
Rostral middle frontal	6.9	Supramarginal	6.9
Pars opercularis	6.9		
Precentral	10.3		
Supramarginal	6.9		
Superior parietal	6.9		

Abbreviations: ICL = intracortical lesion(s); LCL = leukocortical lesion(s); MS = multiple sclerosis. Regions are defined according to the Desikan atlas.

the entire group. This was higher than the ratio of sulci surface to total cortical surface, representing 47% in mean ($p = 10^{-15}$ for ICL and $p = 10^{-2}$ for LCL).

Quantitative T2* in lesional and normal-appearing cortex. As previously reported,[8] in our MS cohort, mean T2* in ICL (41 ± 4.6 ms) and LCL (41.1 ± 3.4 ms) was higher than mean NACGM T2* ($p < 10^{-9}$ by paired t test for ICL and LCL) and than mean cortical T2* in controls ($p < 10^{-6}$ and $p < 10^{-7}$ by linear regression using age and cortical thickness as nuisance factor).

In both RRMS and SPMS subgroups, ICL and LCL had longer T2* relative to NACGM T2* and to cortical T2* in controls. There was no difference in ICL and LCL T2* between RRMS and SPMS (figure 2).

NACGM T2* in patients with MS (34 ± 2.4 ms) was not different from mean cortical T2* (33.03 ± 1.6 ms) in controls. When looking at subgroups, in patients with SPMS only, mean NACGM T2* was higher than mean cortical T2* in controls, and than mean NACGM T2* in RRMS (figure 2).

Extent of ICL and LCL pathology toward perilesional cortex. Figure 3A displays a visual example of geodesic contours surrounding an ICL mask projected on the cortical surface in a patient with RRMS.

In the entire MS cohort, T2* relaxation time was maximum within ICL and LCL (geodesic distance of 0). It remained longer compared with distant perilesional cortex (geodesic distance of 20) up to a geodesic distance of 4 for ICL and 10 for LCL (figure 3B). The actual physical distance between 2 vertices depends on the curvature of the surface. For reference, mean intervertex distance across the whole cortical surface in our population was 0.85 mm (±0.02 SD).

T2* relaxation time surrounding ICL did not differ between RRMS and SPMS, as T2* was still higher up to the same geodesic distance for both groups. However, T2* surrounding LCL decreased closer to

Figure 1 Overlay on "fsaverage" template of cortical lesion probability maps in patients with multiple sclerosis

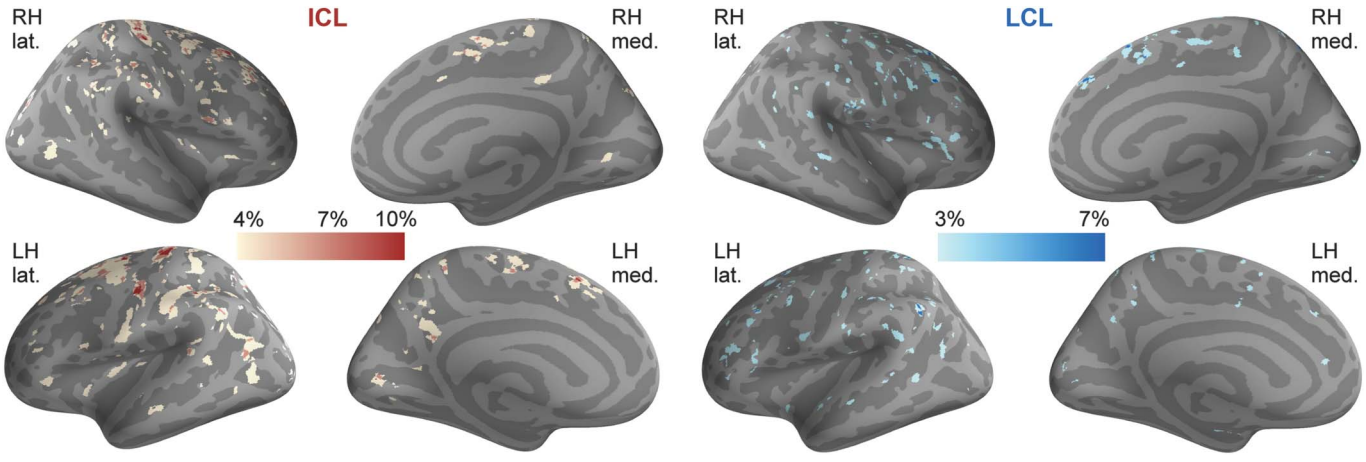

The color overlay represents the vertex-wise frequency of cortical lesion occurrence. ICL = intracortical lesion(s); lat. = lateral; LCL = leukocortical lesion(s); LH = left hemisphere; med. = medial; RH = right hemisphere.

Figure 2 Boxplots of T2* relaxation time (ms) in cortical tissue compartments in controls (green), RRMS (pink), and SPMS (red)

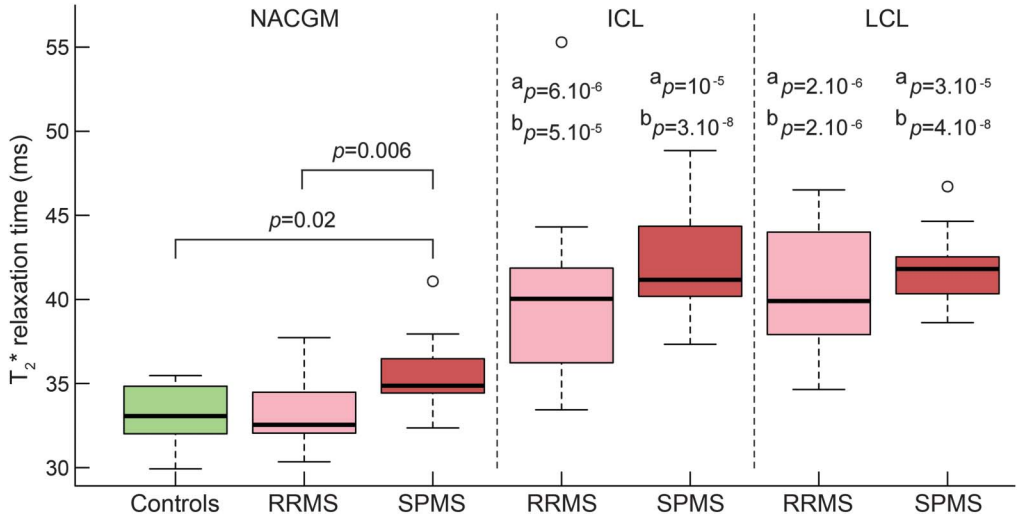

SPMS showed higher NACGM T2* relative to cortical T2* in controls ($p = 0.01$) and NACGM T2* in RRMS ($p = 0.005$), by linear regression including age and cortical thickness as nuisance factors. In RRMS and SPMS, T2* within cortical lesions (ICL and LCL) was higher than NACGM T2* and than control cortex T2*. [a]Statistical significance (p value) of T2* difference between lesional and NACGM within each MS group, by paired t test. [b]Statistical significance (p value) of T2* difference between lesional cortex from patients with MS and cortex from controls, by linear regression including age and cortical thickness as nuisance factor. All p values are corrected for multiple comparisons using false discovery rate. ICL = intracortical lesion(s); LCL = leukocortical lesion(s); MS = multiple sclerosis; NACGM = normal-appearing cortical gray matter; RRMS = relapsing-remitting multiple sclerosis; SPMS = secondary progressive multiple sclerosis.

lesions in the RRMS group compared with the SPMS group.

DISCUSSION We used quantitative T2* MRI at 7T in RRMS and SPMS to characterize spatial and intrinsic tissue characteristics of visible focal CL and NACGM.

ICL, as opposed to LCL, had a preferential pattern of distribution in frontal and parietal lobe, including precuneus, temporal and cingulate cortex, as reported post mortem.[19] A previous in vivo study based on 3T double inversion recovery (DIR) scans on RRMS and primary progressive MS found that CL were preferentially distributed in the frontal lobe, mainly in motor cortex, in the temporal lobe, and anterior cingulate cortex.[20] The authors, however, highlighted that the resolution of their scans did not allow accurate distinction of purely ICL from LCL and juxtacortical lesions. Using ultra-high-resolution scans at 7T (voxel size approximately 0.11 mm^3) to localize CL according to their location across the cortical width, we found that LCL were more randomly distributed than ICL and were mainly localized in frontal and parietal cortex.

The differential distribution pattern between ICL and LCL may reflect, at least in part, different pathogenetic mechanisms underlying ICL and LCL development. Some neuropathologic studies observed that CL, particularly subpial lesions originating from outer cortical layers (defined here as ICL), were located close to foci of meningeal inflammation,[21–23] which suggests that subpial demyelination may be triggered by soluble inflammatory factors originating from the meninges. Lack of association between the 2 processes, however, has also been reported.[24] LCL extend across cortex and WM, and it could be speculated that both inflammatory processes occurring in the meninges and in underlying normal-appearing WM (NAWM) could be at the origin of LCL formation. This could translate into a more widespread distribution pattern, as observed in our cohort. Very little is known about the origin of purely (type II) ICL. Independently from the triggering events that lead to ICL and LCL development, which are still unknown, it is also possible that differences in distribution patterns between CL subtypes underlie different susceptibilities to pathology and/or to remyelination across cortical laminae.[9]

The striking preferential distribution of ICL, and to a lesser extent of LCL, in cortical sulci was observed in some neuropathologic examinations of MS brains.[25] We previously found in patients at different stages of MS diffuse cortical damage as measured by longer T2* and mainly involving cortical sulci. However, the ratio of areas displaying abnormal T2* in sulci relative to gyri ranged from 1 to 2, while in this study, the ratio of focal ICL area belonging to sulci relative to gyri was greater than 5. This

Figure 3 T2* in cortical lesions and perilesional cortex

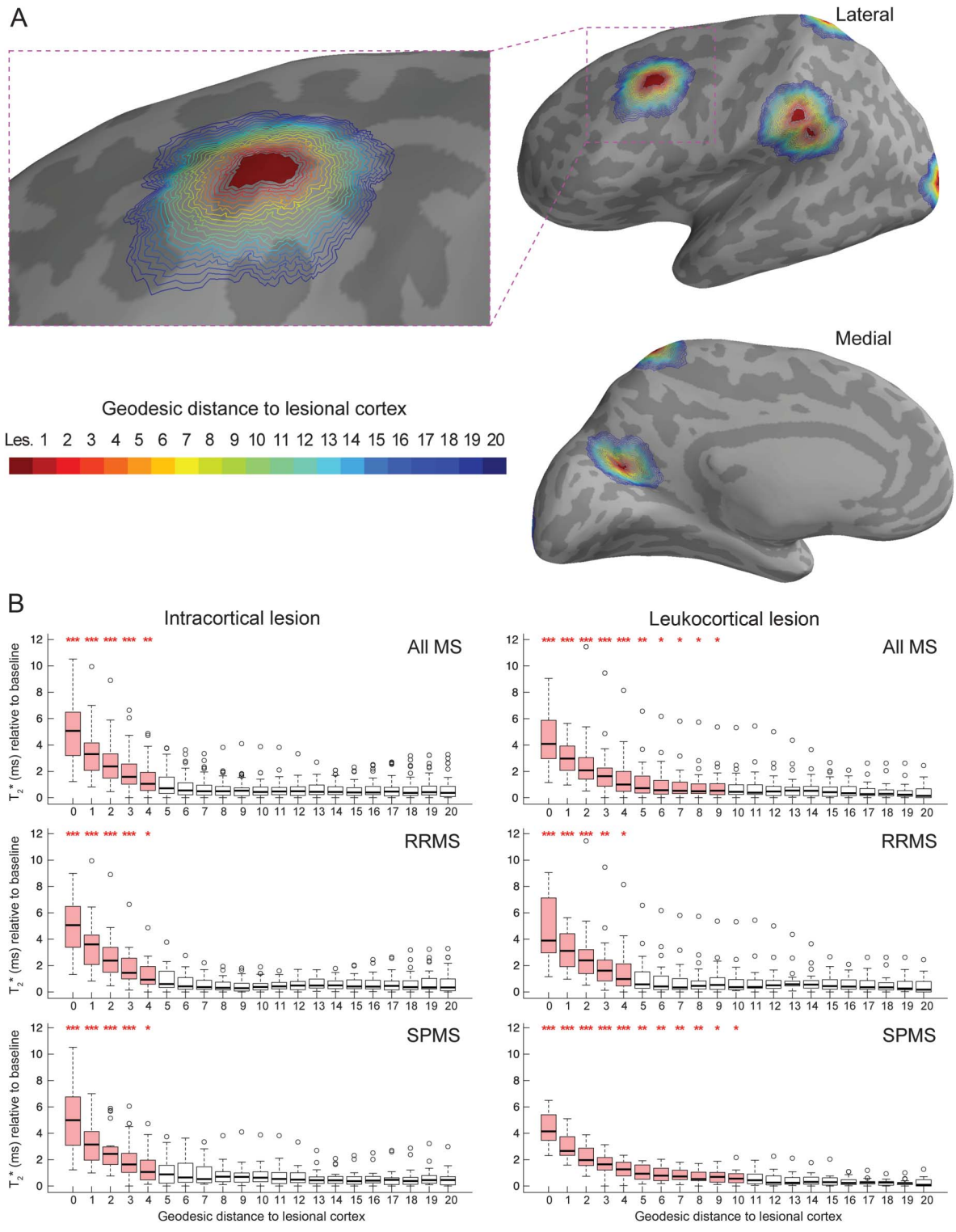

(A) Example of the geodesic distance contour surrounding lesional cortex overlaid on the left hemisphere cortical surface of a patient with RRMS. Binary mask of ICL was projected on the cortical surface, providing a 2-dimensional ICL mask (in red). Perilesional vertices were identified using their geodesic distance from the lesions, each value (1–20) being assigned a different color for visualization purposes. Each cortical lesion mask was analyzed as a whole for each participant, implying that there was no ambiguity when calculating the geodesic distance to lesions that were close to each other as figured in this example. (B) Boxplots of T2* relaxation time (ms) as a function of the geodesic distance from the lesions in all patients with MS, patients with RRMS, and patients with SPMS. T2* is expressed relative to its baseline value in each participant (see methods section). Boxplots in red indicate that there is a difference between mean T2* of the given geodesic distance and mean T2* far from the lesions (geodesic distance of 20) for the specified group of participants. ***$p < 0.001$, **$p < 0.01$, *$p < 0.05$. ICL = intracortical lesion(s); MS = multiple sclerosis; RRMS = relapsing-remitting multiple sclerosis; SPMS = secondary progressive multiple sclerosis.

emphasizes that focal CL themselves may only partly explain the diffuse cortical abnormalities observed in MS.

Although SPMS cases had higher number and volume of CL than RRMS cases, the degree of tissue pathology within CL, as evidenced by longer T2*, was similar throughout MS stages for both lesion subtypes. In contrast, NACGM was diffusively pathologic in SPMS only, although tissue abnormalities occurred in NACGM surrounding focal ICL and LCL in both relapsing-remitting and secondary progressive disease stages. A previous work found global NACGM abnormalities in RRMS, as evidenced by increase in diffusion tensor imaging fractional anisotropy, which correlated with disability.[26] The suboptimal detection of subpial lesions by 3T DIR imaging compared with 7T GRE T2* scans, and the different biological substrates underlying T2* and diffusion metrics abnormalities in the cortex could, at least in part, explain discrepancies between our and previous DIR findings.

Previous imaging studies reported abnormalities surrounding WM lesions, tapering away from lesions toward the NAWM,[27,28] but diffuse NAWM pathology has also been observed independently of focal WM lesions, particularly in progressive MS.[29] We used a surface-based approach to compute quantitative T2* in the cortex as a function of distance from the lesions, using the vertex geometry of the cortical surface in each participant. This method, compared to 3D volume-based approaches, has the advantage of taking into account the circumvolved nature of the cortex, minimizing partial volume effects. We found a gradient of T2*, decreasing from the CL border toward NACGM. Of note, this gradient was larger for LCL than ICL, mainly in SPMS, suggesting that SPMS LCL tend to have a broader destructive pathology surrounding lesions. These findings also suggest that the laminar pathology previously observed throughout stages of MS[8] might be an expression of a more diffuse degenerative process in chronic disease as evidenced postmortem.[7,30] In RRMS, the lack of significant diffuse T2* changes in global NACGM and perilesional cortex (with the exception of cortex in close CL proximity) suggests that cortical pathology mainly resides within focal CL. Since neuropathologic studies tend to skew tissue samples toward late-stage MS, knowledge of cortical pathology in earlier stages is limited and needs further investigation.

In our study, patients with RRMS and SPMS, while matched for age, differed in disease duration because patients with SPMS were younger at disease onset. A previous neuropathologic study[22] found that SPMS cases exhibiting aggressive cortical pathology associated with meningeal inflammation had younger age at disease onset compared with SPMS cases with milder cortical disease. Evidence of meningeal inflammation in MS, however, is still debated. Future studies combining our methods and recent developments to image leptomeningeal inflammation, including postcontrast FLAIR MRI,[31] could help to unravel in vivo the link between meningeal inflammation and different CL subtypes.

Overall, our findings show that cortical demyelination expands beyond focal CL in MS, in close proximity to the lesional compartment in RRMS, and more diffusely, far from lesions, in SPMS. Even if ultra-high-resolution 7T MRI was used for detecting CL, it is possible that the determination of CL borders was not as accurate as in ex vivo assessments, and that some CL were missed at visual inspection of scans. Nevertheless, our data suggest that quantitative measures of global cortical integrity outside visible CL could be a potential biomarker of disease severity and progression in MS. Since it has been observed that the pathologic substrates underlying MRI changes in NAWM vary based on the distance from WM lesions,[32] further studies could also determine whether NACGM T2* abnormalities observed in our cohort reflect different pathologic processes based on distance from lesions.

AUTHOR CONTRIBUTIONS

C. Louapre has contributed to acquisition of data, analysis or interpretation of the data, statistical analysis, and drafting/revising the manuscript for content. S.T.G. has contributed to acquisition of data and analysis or interpretation of the data. C.G. has contributed to acquisition of data and analysis or interpretation of the data. C. Langkammer has contributed to analysis or interpretation of the data and drafting/revising the manuscript for content. J.A.S. has contributed to study concept or design and analysis or interpretation of the data. R.P.K. has contributed to study concept or design, analysis or interpretation of the data, and drafting/revising the manuscript for content. C.M. has contributed to study concept or design, acquisition of data, analysis or interpretation of the data, and drafting/revising the manuscript for content.

STUDY FUNDING

This work was supported by grants from the National MS Society (NMSS 4281-RG-A1 and NMSS RG 4729A2/1), the Claflin Award, and partly by NIH R01NS078322-01-A1, US Army W81XWH-13-1-0122, Shared Instrumentation Grant 1S10RR023043, and National Center for Research Resources (NCRR P41-RR14075).

DISCLOSURE

C. Louapre was supported by a fellowship from ARSEP. S. Govindarajan reports no disclosures relevant to the manuscript. C. Giannì was supported by FISM training fellowship 2012/B/4. C. Langkammer and J. Sloane report no disclosures relevant to the manuscript. R. Kinkel reports personal fees from Genzyme, a Sanofi corp., Biogen Idec, Novartis, and grants from Accelerated Cure Project, outside the present work. C. Mainero reports no disclosures relevant to the manuscript. Go to Neurology.org for full disclosures.

Received March 18, 2015. Accepted in final form July 15, 2015.

REFERENCES

1. Calabrese M, Poretto V, Favaretto A, et al. Cortical lesion load associates with progression of disability in multiple sclerosis. Brain 2012;135:2952–2961.

2. Nielsen AS, Kinkel RP, Madigan N, Tinelli E, Benner T, Mainero C. Contribution of cortical lesion subtypes at 7T MRI to physical and cognitive performance in MS. Neurology 2013;81:641–649.
3. Roosendaal SD, Moraal B, Pouwels PJ, et al. Accumulation of cortical lesions in MS: relation with cognitive impairment. Mult Scler 2009;15:708–714.
4. Mainero C, Benner T, Radding A, et al. In vivo imaging of cortical pathology in multiple sclerosis using ultra-high field MRI. Neurology 2009;73:941–948.
5. Pitt D, Boster A, Pei W, et al. Imaging cortical lesions in multiple sclerosis with ultra-high-field magnetic resonance imaging. Arch Neurol 2010;67:812–818.
6. Yao B, Hametner S, van Gelderen P, et al. 7 Tesla magnetic resonance imaging to detect cortical pathology in multiple sclerosis. PLoS One 2014;9:e108863.
7. Seewann A, Vrenken H, Kooi EJ, et al. Imaging the tip of the iceberg: visualization of cortical lesions in multiple sclerosis. Mult Scler 2011;17:1202–1210.
8. Mainero C, Louapre C, Govindarajan ST, et al. A gradient in cortical pathology in multiple sclerosis by in vivo quantitative 7 T imaging. Brain 2015;138:932–945.
9. Chang A, Staugaitis SM, Dutta R, et al. Cortical remyelination: a new target for repair therapies in multiple sclerosis. Ann Neurol 2012;72:918–926.
10. Polman CH, Reingold SC, Banwell B, et al. Diagnostic criteria for multiple sclerosis: 2010 revisions to the McDonald criteria. Ann Neurol 2011;69:292–302.
11. Bo L, Vedeler CA, Nyland HI, Trapp BD, Mork SJ. Subpial demyelination in the cerebral cortex of multiple sclerosis patients. J Neuropathol Exp Neurol 2003;62:723–732.
12. Kurtzke JF. Rating neurologic impairment in multiple sclerosis: an Expanded Disability Status Scale (EDSS). Neurology 1983;33:1444–1452.
13. Roxburgh RH, Seaman SR, Masterman T, et al. Multiple Sclerosis Severity Score: using disability and disease duration to rate disease severity. Neurology 2005;64:1144–1151.
14. Dale AM, Fischl B, Sereno MI. Cortical surface-based analysis: I: segmentation and surface reconstruction. Neuroimage 1999;9:179–194.
15. Fischl B, Dale AM. Measuring the thickness of the human cerebral cortex from magnetic resonance images. Proc Natl Acad Sci USA 2000;97:11050–11055.
16. Cohen-Adad J, Polimeni JR, Helmer KG, et al. T(2)* mapping and B(0) orientation-dependence at 7 T reveal cyto- and myeloarchitecture organization of the human cortex. Neuroimage 2012;60:1006–1014.
17. Govindarajan ST, Cohen-Adad J, Sormani MP, Fan AP, Louapre C, Mainero C. Reproducibility of T2* mapping in the human cerebral cortex in vivo at 7 tesla MRI. J Magn Reson Imaging 2015;42:290–296.
18. Greve DN, Fischl B. Accurate and robust brain image alignment using boundary-based registration. Neuroimage 2009;48:63–72.
19. Kutzelnigg A, Lassmann H. Cortical demyelination in multiple sclerosis: a substrate for cognitive deficits? J Neurol Sci 2006;245:123–126.
20. Calabrese M, Battaglini M, Giorgio A, et al. Imaging distribution and frequency of cortical lesions in patients with multiple sclerosis. Neurology 2010;75:1234–1240.
21. Lucchinetti CF, Popescu BF, Bunyan RF, et al. Inflammatory cortical demyelination in early multiple sclerosis. N Engl J Med 2011;365:2188–2197.
22. Magliozzi R, Howell O, Vora A, et al. Meningeal B-cell follicles in secondary progressive multiple sclerosis associate with early onset of disease and severe cortical pathology. Brain 2007;130:1089–1104.
23. Magliozzi R, Howell OW, Reeves C, et al. A gradient of neuronal loss and meningeal inflammation in multiple sclerosis. Ann Neurol 2010;68:477–493.
24. Kooi EJ, Geurts JJ, van Horssen J, Bo L, van der Valk P. Meningeal inflammation is not associated with cortical demyelination in chronic multiple sclerosis. J Neuropathol Exp Neurol 2009;68:1021–1028.
25. Howell OW, Reeves CA, Nicholas R, et al. Meningeal inflammation is widespread and linked to cortical pathology in multiple sclerosis. Brain 2011;134:2755–2771.
26. Calabrese M, Rinaldi F, Seppi D, et al. Cortical diffusion-tensor imaging abnormalities in multiple sclerosis: a 3-year longitudinal study. Radiology 2011;261:891–898.
27. Vrenken H, Geurts JJ, Knol DL, et al. Normal-appearing white matter changes vary with distance to lesions in multiple sclerosis. AJNR Am J Neuroradiol 2006;27:2005–2011.
28. Zhang Y, Moore GR, Laule C, et al. Pathological correlates of magnetic resonance imaging texture heterogeneity in multiple sclerosis. Ann Neurol 2013;74:91–99.
29. Kutzelnigg A, Lucchinetti CF, Stadelmann C, et al. Cortical demyelination and diffuse white matter injury in multiple sclerosis. Brain 2005;128:2705–2712.
30. Klaver R, Popescu V, Voorn P, et al. Neuronal and axonal loss in normal-appearing gray matter and subpial lesions in multiple sclerosis. J Neuropathol Exp Neurol 2015;74:453–458.
31. Absinta M, Vuolo L, Rao A, et al. Gadolinium-based MRI characterization of leptomeningeal inflammation in multiple sclerosis. Neurology 2015;85:18–28.
32. Moll NM, Rietsch AM, Thomas S, et al. Multiple sclerosis normal-appearing white matter: pathology-imaging correlations. Ann Neurol 2011;70:764–773.

Beyond focal cortical lesions in MS: An in vivo quantitative and spatial imaging study at 7T

Céline Louapre, Sindhuja T. Govindarajan, Costanza Giannì, et al.

Neurology 2015;85;1702-1709 Published Online before print October 14, 2015
DOI 10.1212/WNL.0000000000002106